

# Soil Microbial Functional Succession Over One Year of Human Decomposition

Allison R. Mason<sup>1</sup>, Lois S. Taylor<sup>2</sup>, Naomi Gilbert<sup>1</sup>,  
Steven W. Wilhelm<sup>1</sup>, Jennifer M. DeBruyn<sup>1,2\*</sup>

<sup>1</sup>Department of Microbiology, University of Tennessee-Knoxville, 1311  
Cumberland Avenue, Knoxville, 37996.

<sup>2</sup>Department of Biosystems Engineering and Soil Science, University of  
Tennessee-Knoxville, 2506 E.J. Chapman Drive, Knoxville, 37996.

\*Corresponding author(s). E-mail(s): [jdebruyn@utk.edu](mailto:jdebruyn@utk.edu);

## Abstract

**Background** The succession of microbial communities during vertebrate decomposition has been observed in various settings, documenting changes in taxa as decomposition progresses. These studies have predominantly employed phylogenetic markers (*i.e.*, rRNA genes), describing community composition and structure, but ultimately are not informative of which members are active or metabolic pathways they might be expressing. This has left a foundational knowledge gap regarding the functional roles of microorganisms in vertebrate decomposition, which ultimately impact ecosystem functioning. Here we present the first known study investigating gene expression in soil impacted by human decomposition in a terrestrial ecosystem. Total RNA was extracted and meta-transcriptomes obtained from soil samples collected over the course of one year from below three decomposing human bodies.

**Results** Microbial gene expression profiles shifted in response to decomposition: decomposition impacted soils were most different from controls (*i.e.* nearby soils unimpacted by decomposition) at day 86, and profiles remained altered even

after one year. Shifts in gene expression were partially explained by environmental and soil physiochemical variables, including internal body accumulated degree hours ( $p = 0.001$ ), as well as soil temperature ( $p = 0.045$ ), pH ( $p = 0.042$ ) and electrical conductivity ( $p = 0.037$ ). Differential expression analysis revealed that microbes in decomposition soils displayed increased expression of stress response genes (mean fold change 3.48), particularly heat shock proteins ( $p < 0.001$ ), whose expression increased between days 0 and 58 and remained elevated through day 376. Further, we identified genes whose expression was altered at certain timepoints. This included increased expression of genes encoding hydroxylamine oxidoreductase (HAO) (85x), nitric oxide reductase (83x), and nitrous oxide reductase (19x) at day 86 when dissolved oxygen was ~85%, suggesting that microbial communities may be converting hydroxylamine to nitric oxide and reducing nitrous oxide to nitrogen gas during reduced oxygen conditions.

**Conclusions** Our results show that human decomposition alters soil microbial gene expression profiles providing evidence of altered microbial metabolisms (*e.g.*, taurine metabolism, nitrogen cycling, and lipid metabolism) and reveal the potential of vertebrate decomposition to have both ephemeral and lasting effects on ecosystem processing in response to mortality events.

**Keywords:** Human Decomposition, Microbial Succession, Metatranscriptomics, Soil Microbial Ecology

## Introduction

Soil microbial communities are important drivers of ecosystem processes in terrestrial environments. Many soil microbes are decomposers that are involved in degradation of complex organic matter and drive nutrient cycling in terrestrial ecosystems. Environmental disturbances can impact the presence and/or activity of soil microorganisms that are involved in these cycles, ultimately affecting nutrient availability and the release of greenhouse gas emissions, such as CO<sub>2</sub> and N<sub>2</sub>O [1, 2]. Vertebrate death and subsequent carcass deposition in terrestrial ecosystems is one disturbance resulting in the deposition of large quantities of organic C and N [3–10], along with other elements (P, K, S, *etc*) [11], which collectively contribute to microbially-mediated

biogeochemical cycling. In addition to this, changes in pH, temperature, and fluctuations in soil oxygen provide abiotic filtering further impacting microbial metabolic strategies [7–9, 11, 12].

While C and N transformations have been documented during decomposition, the functional response of microbes and their roles in nutrient cycles remain unclear. The composition and structure of decomposition-impacted soil microbial communities have been investigated using amplicon sequencing of marker genes (*i.e.*, 16S rRNA, 18S rRNA, ITS), revealing successional dynamics [13]. This has allowed us to investigate changes in microbial biodiversity and composition in response to vertebrate decomposition, revealing patterns such as increases in the anaerobic taxa *Firmicutes* and *Bacteroidetes*. However, few studies have investigated soil biogeochemistry and microbial communities within the same study, which can further help to describe microbial ecology in human and animal decomposition systems. Taylor et al. (2024) [14] suggested that fungal community shifts were linked to changes in soil dissolved oxygen, highlighting interactions between soil microbes and the surrounding environment. While insightful for making potential connections between taxa and physiochemistry, these analyses cannot inform which taxa are active members of the community responsible for chemical transformations, which functional pathways/genes are expressed, and how these pathways are altered in response to decomposition.

Methods such as RNA sequencing (*i.e.*, metatranscriptomics) and metabolomics can be used to investigate microbial community functional succession in response to decomposition by measuring gene expression and metabolites, respectively. This can inform how ecological functions, including C and N cycling, are impacted by decomposition events in terrestrial ecosystems. To date, only two studies have applied metatranscriptomic approaches to assess mRNA in vertebrate decomposition samples [15, 16]:

Burcham et al. (2019) [15] examined gene expression of internal organ microbial communities during mouse decomposition, while Ashe et al. (2021) [16] examined gene expression of oral microbial communities during human decomposition. Both studies suggest that the host microbial community functionality is altered during decomposition, including differential expression of amino acid and carbohydrate metabolism in the heart [15] and shifts in gene transcripts across different taxa [16]. We expect that soil microbial community gene expression profiles are also altered; however, this has never been examined to our knowledge. The decomposition-impacted soil metabolome was assessed by DeBruyn et al. (2021) [17], showing changes in soil metabolites over time including increased prevalence of amino acids, however it is unclear which microbes are responsible for these shifts. Additionally, DeBruyn et al. (2021) [17] showed the soil metabolome was still altered compared to starting conditions at the end of the 21-week study, suggesting long-term impacts of decomposition on soil microbial functioning.

The purpose of this study was to investigate soil microbial gene expression during a one-year period of human decomposition and address the following questions: (1) which genes are differentially expressed in soils impacted by human decomposition? (2) how does gene expression change over time in decomposition-impacted soils? (3) do microbial gene expression profiles return to pre-decomposition conditions after one year? The human body is comprised of nutrient-rich organic molecules, many of which are broken down during decomposition. We hypothesized that gene expression would change over time as resources are used and transformed and soil chemical and physical conditions change due to the influx of decomposition products [8, 9, 17]. For example, we expected to observe changes in the expression of genes encoding enzymes involved in nitrogen cycling, as changes in nitrogen pools have been previously described in decomposition soils [8]. Of the main macromolecules in the body (carbohydrates, proteins, lipids, and nucleic acids), we were particularly interested in

lipid metabolism, as we expect lipids from the body to enter the soil during decomposition and previous studies showed an increase of lipolytic organisms in decomposition soils [12, 18]. Finally, multiple studies have shown that soil chemistry [5, 8] and microbial community composition [19, 20] (via 16S rRNA gene amplicon sequencing) are still impacted after one year, therefore we did not expect soil expression profiles to return to pre-decomposition conditions.

To answer these questions, metatranscriptomes of soil samples collected at six key timepoints over one year of human decomposition were used to determine the active populations and expression of genes and pathways relevant to the enhanced biogeochemical cycling observed in decomposition hotspots. We compared gene expression between decomposition timepoints and control soils that were unexposed to decomposition products to identify functions or functional pathways of interest. This assessment of functional profiles within decomposition-impacted soils provided insight into the microbial response to vertebrate decomposition in terrestrial settings and biogeochemical cycling within these hotspots.

## Results

### Soil Physiochemistry

Soil chemistry was altered in response to human decomposition, with multiple parameters still impacted after one year [14]. Generally, soil pH decreased and remained low in decomposition soils of all but one individual. Soil electrical conductivity (EC) increased in response to decomposition, remaining elevated through approximately day 58 before gradually decreasing throughout the remainder of the study (Supplementary Material 1). Respiration (evolved CO<sub>2</sub>) increased by an order of magnitude beginning at day 12, which corresponded to a reduction in soil dissolved oxygen (DO)

231 to 29% - 48.9%. Ammonium concentrations increased 78-fold, reaching maximum con-  
232 centrations between days 12 and 58. This was followed by decreased ammonium and  
233 increased nitrate concentrations at day 86, with nitrate concentrations reaching a  
234 maximum at day 168 (Supplementary Material 1).  
235  
236

237

238

## 239 Sequencing

240

241 Illumina sequencing of the 24 libraries yielded a total of 5,073,476,730 reads, or  
242 2,536,738,365 paired reads, with a mean of 105,697,432 paired reads per sample.  
243

244 Removal of adapters and low-quality reads removed 4.7% of all reads, leaving  
245 4,834,123,062 total reads. Filtering of ribosomal RNA further removed 7.3% of reads,  
246 leaving 4,479,804,360 reads for assembly. After co-assembly, a total of 6,257,674 pro-  
247 teins were identified by Prodigal. From this, 1,048,573 proteins were annotated by  
248

249 eggNOG-mapper (16.7%). Most of the annotated proteins were taxonomically anno-  
250 tated as bacteria (91.3%), followed by eukaryotes (7.6 %), and archaea (0.81 %). Of  
251 the 7.6% of eukaryotic proteins, 64.4% (4.9% of all proteins) were annotated as fungi.  
252  
253

254 For this study, genes of interest included all bacterial, archaeal, and fungal proteins,  
255 therefore all non-fungal eukaryotic proteins (32,004) were removed prior to down-  
256 stream analysis. The reference file of genes was then used to determine gene transcript  
257 counts in all samples using CLC genomic workbench. The percent of reads mapped  
258 to genes of interest ranged from 21% to 38%, with an average of 31% reads mapped.  
259

260 Gene counts were then combined in a single file and used for downstream analyses in  
261

262 R.  
263  
264

265

266

267

268

## 269 Microbial gene expression in response to human decomposition

270

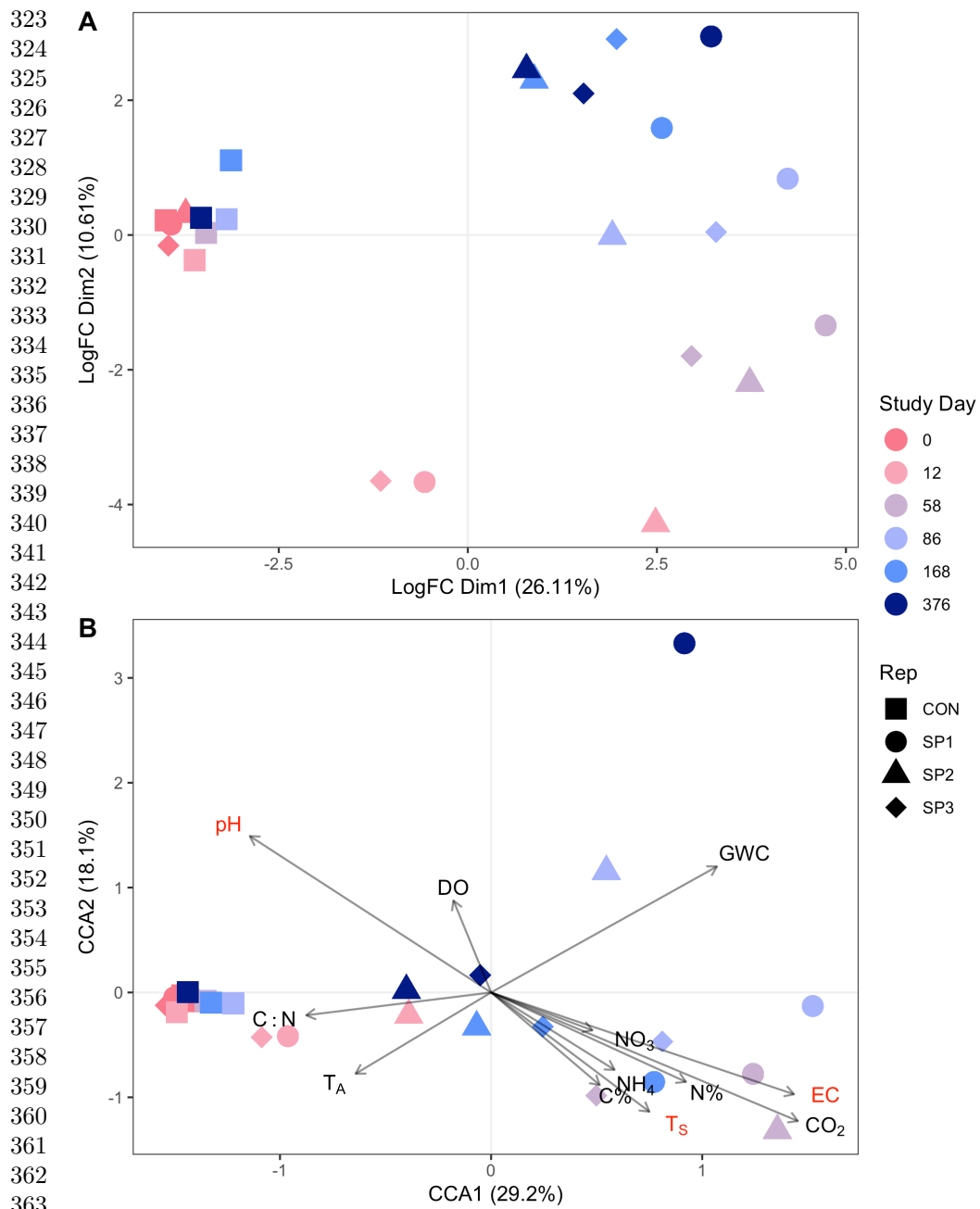
271 Gene expression profiles in decomposition-impacted soils shifted away from controls  
272 and day zero samples as decomposition progressed (Fig 1A). Expression was most  
273 different from controls on study days 58, 86, 168 (Supplementary Material 2), before  
274

275

276

shifting back toward control conditions on study day 376. After one year of decomposition, soil gene expression profiles had not returned to pre-decomposition conditions, as evidenced by their clustering away from controls and day zero samples in the MDS plot (Fig 1A).

**Figure 1: Microbial gene expression profiles are altered during human decomposition.** Multidimensional scaling (MDS) shows gene expression within soils changed as decomposition progressed (A). Additionally, canonical correspondence analysis (CCA) shows that environmental variables explained 47.3% of the variation in gene expression profiles (B). Variables in bold red type significantly ( $p < 0.05$ ) explained some of the variation in gene expression profiles as assessed by Permutational Analysis of Variance (PERMANOVA). In both panels soils from controls (CON) and the three donors (SP1, SP2, SP3) are denoted by symbol shape, while color represents study day. In B, soil physiochemical variable loadings are represented by arrows: Gravimetric water content (GWC), electrical conductivity (EC), pH (pH), dissolved oxygen (DO), respiration (evolved  $\text{CO}_2$   $\mu\text{mol gdw}^{-1}$ ), ammonium ( $\text{NH}_4$ ), and nitrate ( $\text{NO}_3$ ) concentrations ( $\text{mg gdw}^{-1}$ ), percent carbon (%C), percent nitrogen (%N), carbon:nitrogen ratio (C:N), ambient temperature ( $T_A$ ), and soil temperature ( $T_S$ ).



Some correlations were observed between gene expression shifts and soil physiochemical data at decomposition timepoints. Canonical correspondence analysis (CCA) was

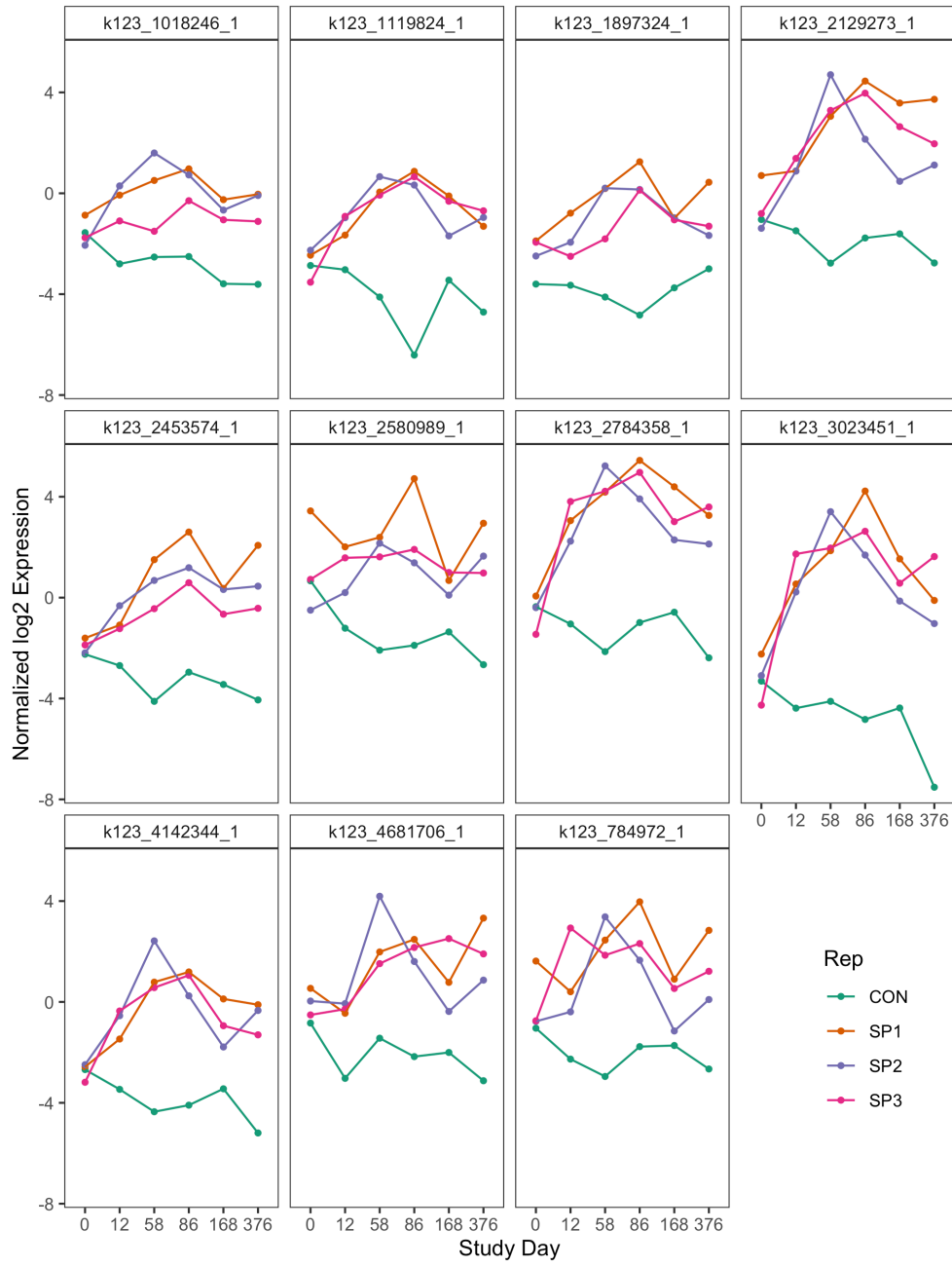


used to constrain gene expression data with soil physiochemical data (Fig 1B). CCA1 and CCA2 explained 29.2% and 18.1% of the variance in gene expression, respectively. Transcript profiles at day 12 were associated with an increase in soil carbon to nitrogen ratio (C:N). Gene expression profiles at days 58 to 86 were positively correlated with increased soil temperature, EC, and evolved CO<sub>2</sub>, while study day 168 was associated with elevated levels of soil NO<sub>3</sub>. Further, Permutational Analysis of Variance (PERMANOVA) revealed that internal accumulated degree hours (ADH), soil temperature, pH, and EC significantly explained some of the variation in gene expression profiles ( $p < 0.05$ ). No other soil chemical variables were significant at  $\alpha = 0.05$  (Supplementary Material 3).

Overall, decomposition changed soil gene expression profiles over the one-year study relative to control soils. Differential expression analysis between decomposition and control soils identified 7,047 down-regulated and 38,425 up-regulated genes. Gene transcripts that were associated with control soils belonged to a wide variety of clusters of orthologous genes (COG) functional categories. Specifically, the top 20 genes whose expression was higher in control soils belonged to ten unique COG categories, including signal transduction mechanisms, transcription, and those of unknown function. In contrast, the top 20 genes whose expression was higher in decomposition soils only fell into four COG categories (Supplementary Material 4 A): 1) post-translational modification, protein turnover, and chaperones; 2) energy production and conversion; 3) cell motility; and 4) carbohydrate transport and metabolism. The most common COG category represented in decomposition soils (80% of the top 20 genes) was post-translational modification, protein turnover, and chaperones. Within this category, several heat shock stress response genes were identified, including SSA2, HSP82, and clpB (Supplementary Material 5). Further investigation into these genes shows their expression increased in response to decomposition, typically reaching maximum transcript levels around study days 58 and 86 (Fig 2). This corresponded to elevated soil

temperatures below decomposing bodies between study days 12-80, with soil temperatures increasing to approximately 43°C [14], and maximum soil EC and minimum dissolved oxygen measurements between days 12 and 58 (Supplementary Material 1).

**Figure 2: Normalized log2 expression of heat shock proteins identified by differential expression analysis comparing decomposition and control soils.** Each panel represents a single heat shock transcript, labeled with query ID. Symbol color denotes if the sample is a control (CON, green), or one of three individuals: SP1 (orange), SP2 (purple), or SP3 (pink).



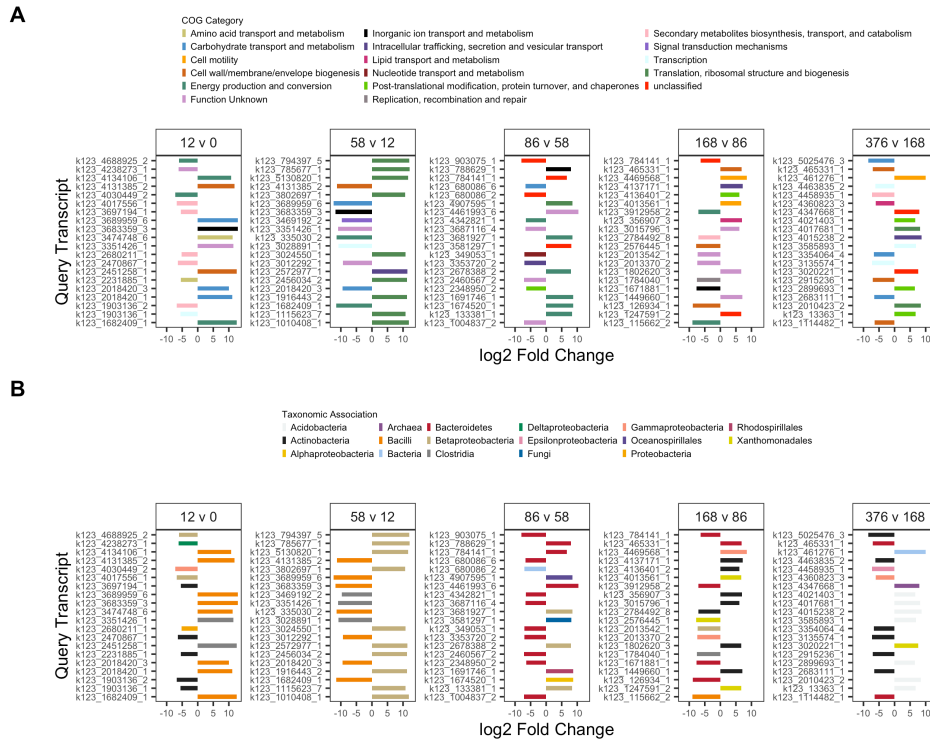
Taxonomy associated with top differentially expressed gene transcripts also differed between control and decomposition soils. The top 40 significantly differentially

expressed gene transcripts in decomposition soils were associated with Fungi, *Actinobacteria*, and *Xanthomonadales*, while gene transcripts in controls were associated with *Acidobacteria*, *Cyanobacteria*, *Proteobacteria* ( $\alpha$ ,  $\delta$ ,  $\gamma$ ), and Planctomycetes (Supplementary Material 4 B). The greatest number of differentially expressed genes relative to control samples was observed at day 86, where we saw 145,460 and 124,883 up- and down-regulated genes, respectively.

## Fate of decomposition products as evidenced in gene expression profiles over time

Differential expression analysis between respective sequential study days further revealed which genes were altered between decomposition timepoints. The top ten significantly up- and down-regulated genes, determined by the lowest p-values from differential expression analysis ( $< 0.05$ ), are reported in Supplementary Material 6 and Fig 3.

**Figure 3: Top twenty up- and down-regulated genes in decomposition soils comparing sequential study days (0, 12, 58, 86, 168, 376) colored by COG functional category (A) and taxonomic annotation (B).** Positive values denote increased expression compared to the preceding timepoint, while negative values denote a decrease.



Expression of genes annotated with the COG categories cell wall/membrane/envelope biogenesis, inorganic ion transport and metabolism, and carbohydrate transport and metabolism increased from day 0 to 12. In contrast, expression of secondary metabolite biosynthesis, transport, and catabolism genes decreased during this period (Fig 3A). Transcripts from *Bacilli* and *Clostridia* increased, while transcripts from *Actinobacteria* decreased between study days zero and 12 (Fig 3).

Between days 12 and 58, 90% of the topmost upregulated genes were associated with the translation, ribosomal structure and biogenesis COG and all were taxonomically associated with *Betaproteobacteria* (Fig 3A,B). Many of these genes were annotated as ribosomal protein large (RPL), involved in ribosomal binding. Genes across multiple COG categories with taxonomic associations to *Bacilli* and *Clostridia* decreased

599 between study days 12 and 58, six of which were transcripts that previously increased  
600  
601 between days zero and 12 (Fig 3B, Supplementary Material 6).

602  
603 Multiple transcripts associated with the energy production and conversion COG, as  
604  
605 well as transcripts annotated with the COGs inorganic transport and metabolism,  
606  
607 and translation, ribosomal structure and biogenesis, increased between days 58 and  
608 86 (Fig 3A). Two of the upregulated energy and production and conservation tran-  
609  
610 scripts were associated with cytochrome c oxidase subunits in *Betaproteobacteria*,  
611  
612 while another was annotated as *hao*, encoding the enzyme hydroxylamine dehydroge-  
613  
614 nase which is involved in conversion of hydroxylamine to nitrite during nitrification  
615 (Supplementary Material 6). Further investigation into hydroxylamine dehydrogenase  
616  
617 showed a significant increase in *hao* transcripts at day 86 followed by subsequent  
618  
619 decreases at days 168 and 376 ( $F = 4.183$ ;  $p = 0.02$ ). This increase corresponded to  
620  
621 decreased soil ammonium levels and subsequent accumulation of nitrate (Supplemen-  
622  
623 tary Material 1). Half of the topmost downregulated genes between days 58 and 86  
624  
625 were not assigned to a COG (*i.e.*, unclassified) or were of unknown function.

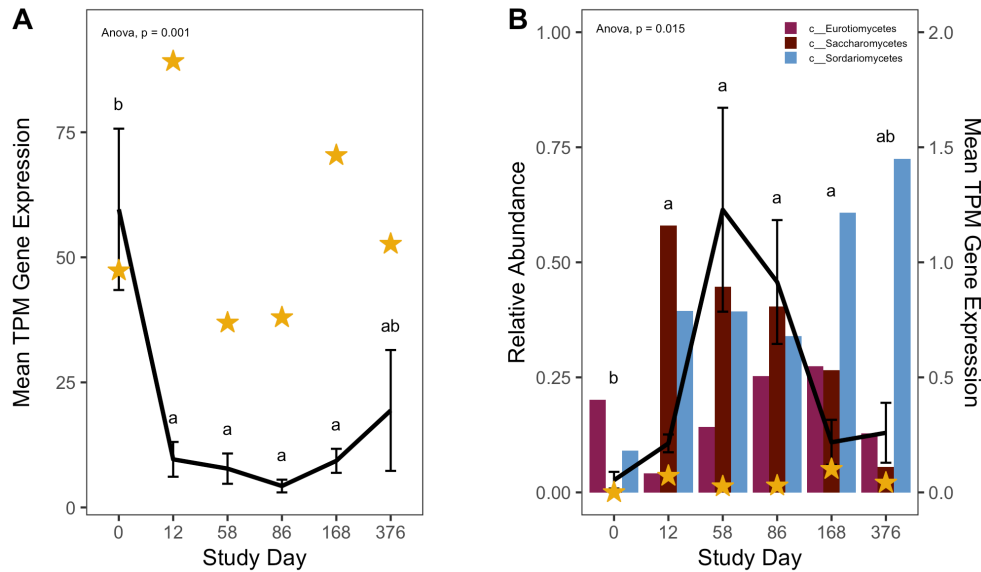
626  
627 Differential expression comparing study days 86 with 168 and 168 with 376 identified  
628  
629 genes across a variety of functional categories, with many unclassified in the COG  
630  
631 database or with unknown function (Fig 3A). Expression of carbohydrate transport  
632  
633 and metabolism genes associated with *Bacilli* decreased between day 168 and 376.  
634  
635 *Acidobacteria* transcripts increased in decomposition-impacted soils between study  
636  
637 day 168 and 376, but were not associated with any single COG category (Fig 3B).

## 637 Carbon compound metabolism

638  
639 We expected to observe increased expression of lipid metabolizing genes during active  
640  
641 and advanced decomposition as microbes degraded lipids deposited in the soil [18].  
642  
643  
644

Therefore, we investigated changes in triacylglycerol lipase (enzyme commission number: 3.1.1.3) gene transcription in our soils. Generally, lipase transcripts decreased as decomposition progressed (HLM  $F = 6.564$ ,  $p < 0.001$ ), however we also observed a significant interaction between study day and taxonomic annotation ( $F = 8.786$ ;  $p < 0.001$ ). Specifically, lipase gene transcripts annotated as bacteria decreased with decomposition time ( $F = 10.392$ ;  $p = 0.001$ ), while fungal lipase transcripts increased, reaching a maximum at study day 58 ( $F = 4.509$ ;  $p = 0.015$ ) (Fig 4).

**Figure 4: Mean transcript abundance, in transcripts per million (TPM), of all bacterial (A) and fungal (B) triacylglycerol lipase (EC 3.1.1.3) genes over time.** Black lines (A, B) report mean and standard deviation of TPM from three individuals (black line), while gold stars denote mean TPM in control soils. P-values are the result of ANOVAs where average TPM and study day are the dependent and independent variables, respectively, while letters are the result of post-hoc Tukey tests between decomposition timepoints. In B, bars show the relative abundance of the fungal classes *Saccharomycetes*, *Sordariomycetes*, and *Eurotiomycetes*, reported in Taylor et al. (2024).

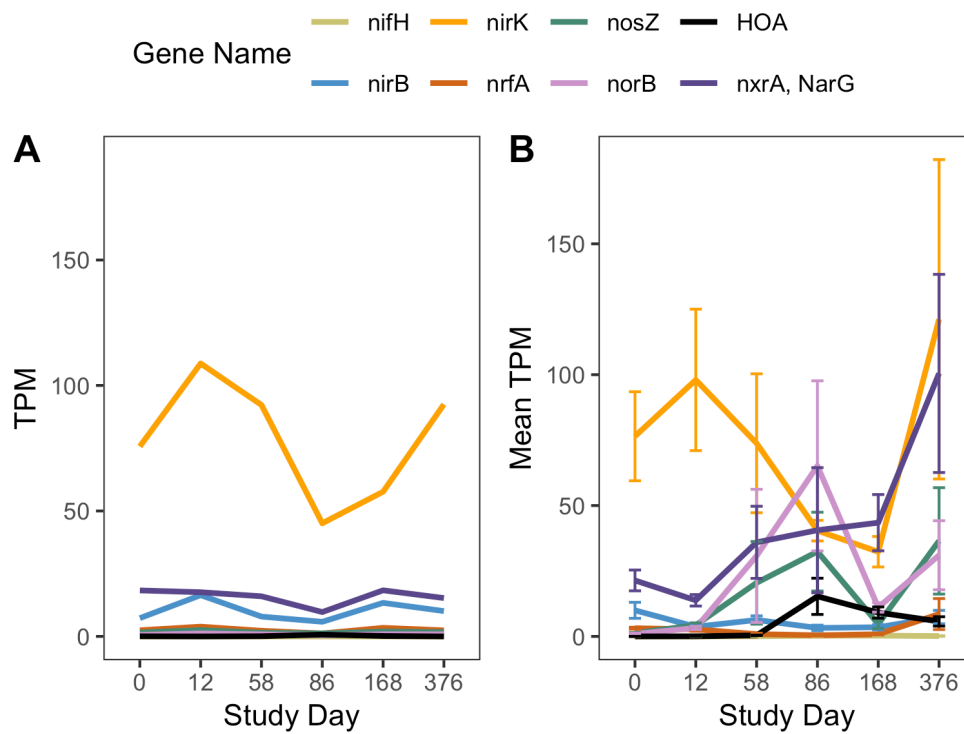


## Nitrogen- and sulfur compound transformations

Expression of nitrogen cycling genes was impacted in response to human decomposition. Due to the detection of *hao* in our differential expression analysis, and our hypotheses predicting changes to nitrogen transformation processes, the expression of genes encoding common enzymes involved in nitrogen cycling (*nifH*, *nirB*, *nirK*, *norB*, *nosZ*, *nrfA*, *nrrA*, and *amoA*) were assessed using their enzyme commission numbers (Fig 5A,B). *nifH*, encoding a subunit of nitrogenase which is involved in nitrogen fixation, displayed little to no changes in gene expression between control and decomposition soils. Transcripts for two genes encoding enzymes contributing to the last two steps of denitrification, *norB* (encodes nitric oxide reductase) and *nosZ* (encodes nitrous oxide reductase), increased between study days 12 and 86, and decreased at study day 168 before increasing again at day 376. In contrast, expression of genes encoding nitrate reductase, *narG*, and NO-forming nitrite reductase, *nirK*, remained low until day 376 when transcripts for both genes increased. As noted above, expression of *hao*, encoding hydroxylamine dehydrogenase, increased at study day 86 before decreasing at remaining timepoints (Fig 3A, Fig 5B). Expression of *amoA*, encoding a subunit of ammonia monooxygenase, and *nrrA*, encoding a subunit of nitrite oxidoreductase, which are involved in nitrification, changed in response to decomposition. *amoA* transcripts initially decreased at day 12, remaining reduced until study day 376. Similarly, abundance of genes that encode for enzymes involved in dissimilatory nitrate reduction, *nirB*, and *nrfA*, was low for the first 168 days, with *nrfA* expression increasing at day 376 (Fig 5B).

**Figure 5: Mean gene expression, in transcripts per million (TPM), of commonly used marker genes for enzymes involved in nitrogen cycling over time in controls (A) and decomposition (B) soils.** Data in B represent mean and standard deviation of TPM from three individuals.

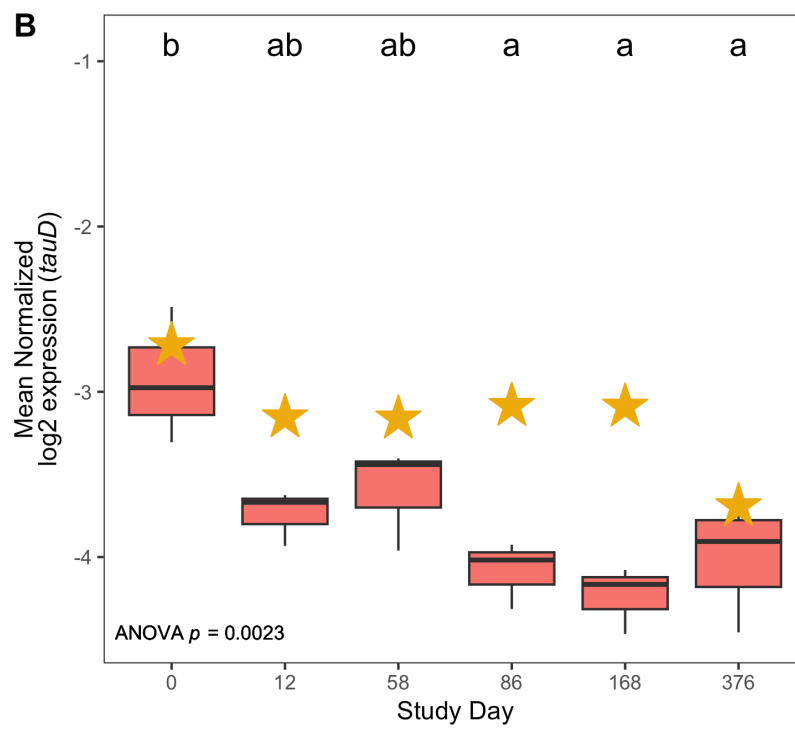
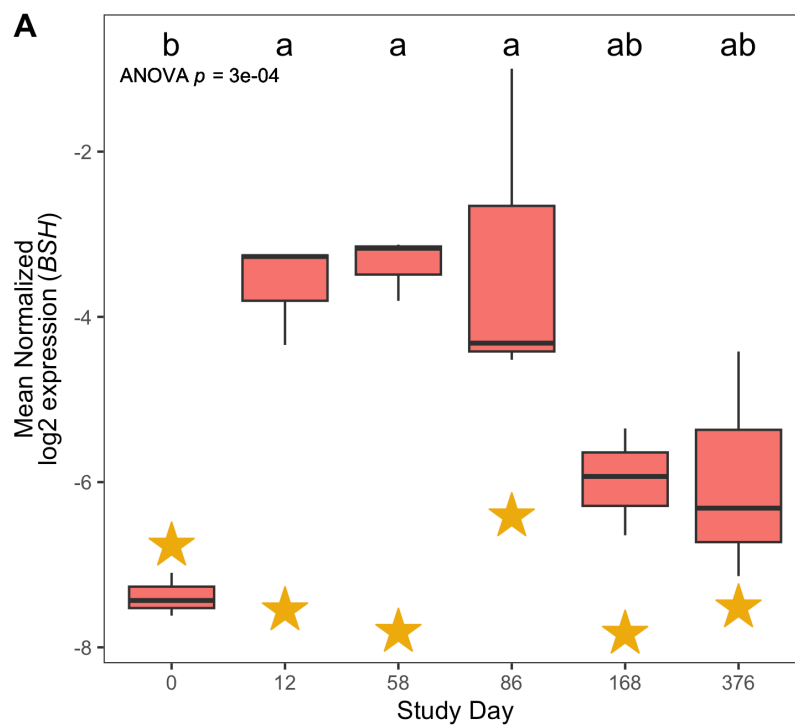




Expression of genes involved in metabolism of nitrogen and sulfur-containing compounds were also impacted by human decomposition. Specifically, four of the top ten genes whose expression decreased at day 12 were related to taurine metabolism, with their annotations associated with *tauD*, encoding taurine dioxygenase. (Supplementary Material 6). Further investigation into *tauD* showed that mean expression of these genes decreased steadily over one year, beginning at day 12 (Fig 6B); however, *tauD* expression in response to human decomposition was variable across taxonomic associations. Most *tauD* transcripts were associated with *Gammaproteobacteria*, *Actinobacteria*, *Betaproteobacteria*, *Alphaproteobacteria*, and fungi. While a majority of the *tauD* gene queries displayed reduced expression over time, expression of fungal-associated and a few *Betaproteobacteria*-associated *tauD* genes increased at day 58 (Supplementary Material 7). Sources of taurine in the human body include taurine

absorbed from the diet and taurine produced from anaerobic microbial deconjugation of bile salts via bile salt hydrolase (BSH) enzymes [21]. Therefore, we also looked at expression of genes encoding BSH enzymes in decomposition soils. Expression of these genes was elevated at days 12, 58, and 86 before converging toward pre-decomposition levels at days 168 and 376 (Fig 6A). Hierarchical linear mixed effects (HLM) models showed that both *tauD* (HLM  $F = 7.356$ ,  $p = 0.002$ ) and BSH ( $F = 13.768$ ,  $p < 0.001$ ) gene expression was significantly different over time (Fig 6A,B).

**Figure 6: Mean bile salt hydrolase, BSH, (A) and *tauD*, taurine dioxygenase, (B) log2 normalized expression in controls (gold stars) and decomposition (boxplots) soils.** Boxplots display the 25th and 75th quartiles and median log2 normalized values between all three individuals at each timepoint. ANOVA p-value is the result of a hierarchical linear mixed effects model accounting for repeated measures of each donor block, while letters denote the results of *post-hoc* Tukey test.



## Discussion

The goal of this study was to assess soil microbial gene expression in response to human decomposition. Metatranscriptomics were applied to soil samples collected over one year from below three decomposing human bodies. From this, we found that microbial gene expression shifted over time, with samples reproducible between individuals. Additionally, we showed that gene expression profiles had not recovered to pre-decomposition conditions after one year. Comparison of control and decomposition expression profiles revealed that heat-shock proteins were elevated in response to decomposition. We also described expression patterns between decomposition timepoints, noting changes in functional gene categories at certain timepoints, in particular with respect to lipid, nitrogen and sulfur metabolism.

### Decomposition impacted soil community gene expression, even after a year

Gene expression profiles remained altered after one year of decomposition. It is unclear if soil microbial communities, in terms of gene expression profiles, have reached a new steady state as a result of decomposition, or if they would eventually return to pre-decomposition conditions. The soil pH, EC,  $\text{NH}_4^+$ ,  $\text{NO}_3^-$ , and total nitrogen (TN) exhibited differences (although not statistical) in these soils following a year of decomposition, however bacterial and fungal community structures, as assessed by rRNA amplicon libraries, were still altered [14]. This indicates that decomposition can continue to structure microbial communities and impact their function for extended periods of time. While nutrient pools and communities both demonstrate less rapid change at later time points in the study, there is not evidence suggesting an arrival at a steady-state post-disturbance microbial community. In some studies, human decomposition can result in elevated carbon and nutrients (organic nitrogen, ammonium, nitrate, and phosphate) for longer than a year [3], suggesting decomposition events

have long lasting effects on the local ecosystem. Together, this has implications for terrestrial ecosystem processing (*e.g.*, nutrient cycling, emission of greenhouse gasses, etc.), as we show that decomposition alters functional metabolism pathways within soil microbial communities. Further work with extended sample collections beyond one year are needed to address how long microbial communities and their functions are impacted.

Bacteria, fungi, and archaea were all represented in expressed genes throughout decomposition, suggesting that members of all three domains have the potential to contribute to decomposition processes and nutrient cycling. While a majority of annotated transcripts were identified as bacteria, fungal transcripts were the second most abundant group. Fungal transcripts made up almost half (seven of the top 15) of the significantly differentially expressed genes associated with decomposition-impacted soils. Additionally, with respect to expression shifts between decomposition time-points, fungal transcripts were among the topmost upregulated genes at study day 86. The presence of fungal transcripts is not surprising as fungi are key decomposers, involved in the degradation of organic matter in terrestrial ecosystems [22]. It was interesting to see an increase in certain fungal transcripts, such as lipase, at study days 58 and 86 when soil oxygen began to recover. We would expect lipids to enter the soil as tissues are broken down during decomposition, so we were surprised to see bacterial lipase genes decrease during decomposition. This suggests that microbial activity in decomposition soils may be constrained by the changing chemical environment, potentially altered oxygen levels in the case of bacterial lipase gene expression. Prior work with these soils showed that soil oxygen concentration was a key driver of changes in both bacterial and fungal community composition [14].

967 **Increased stress responses during decomposition**

968

969 Soil microbial communities expressed stress response genes in response to human  
970 decomposition. Differential expression analysis identified increased expression of mul-  
971 tiple heat shock proteins associated with the taxa *Xanthomonadales*, *Actinobacteria*,  
972 and fungi. Upon further investigation, expression of these genes increased through day  
973 58 and remained high for the remainder of the year. Soil temperature was elevated rel-  
974 ative to controls between study days 8 and 80, with maximum temperatures  $>40^{\circ}\text{C}$ ,  
975 while soil electrical conductivity increased up to 663  $\mu\text{S}/\text{cm}$  (16X higher than back-  
976 ground) through day 58 before slowly decreasing through the remainder of the study.  
977 Soil electrical conductivity (correlates with ionic strength [23] and can indicate soil  
978 salinity) has previously been shown to increase in decomposition soils [8–10, 14]. As  
979 a result, we would expect these microbes to be experiencing both heat and osmotic  
980 stress during this period. Prior work has observed increased heat shock gene expres-  
981 sion during salt stress in paddy soils [24] and the presence of both heat and osmotic  
982 stress genes in desert soils along a salt gradient [25], suggesting saline conditions can  
983 alter the expression of heat and/or osmotic stress genes. In our study we observed  
984 that stress response within soil microbial communities is stimulated during human  
985 decomposition, however, at this time, it is unclear if expression of these genes is in  
986 response to heat stress alone, or in combination with osmotic stress.

987

988

989

990

991

992

993

994

995

996

997

998

999

1000

1001

1002

1003

1004

1005

1006

1007

1008

1009

1010

1011

1012

1013

1014

1015

1016

1017

1018

1019

1020

1021

1022

1023

1024

1025

1026

1027

1028

1029

1030

1031

1032

1033

1034

1035

1036

1037

1038

1039

1040

1041

1042

1043

1044

1045

1046

1047

1048

1049

1050

1051

1052

1053

1054

1055

1056

1057

1058

1059

1060

1061

1062

1063

1064

1065

1066

1067

1068

1069

1070

1071

1072

1073

1074

1075

1076

1077

1078

1079

1080

1081

1082

1083

1084

1085

1086

1087

1088

1089

1090

1091

1092

1093

1094

1095

1096

1097

1098

1099

1100

1101

1102

1103

1104

1105

1106

1107

1108

1109

1110

1111

1112

1113

1114

1115

1116

1117

1118

1119

1120

1121

1122

1123

1124

1125

1126

1127

1128

1129

1130

1131

1132

1133

1134

1135

1136

1137

1138

1139

1140

1141

1142

1143

1144

1145

1146

1147

1148

1149

1150

1151

1152

1153

1154

1155

1156

1157

1158

1159

1160

1161

1162

1163

1164

1165

1166

1167

1168

1169

1170

1171

1172

1173

1174

1175

1176

1177

1178

1179

1180

1181

1182

1183

1184

1185

1186

1187

1188

1189

1190

1191

1192

1193

1194

1195

1196

1197

1198

1199

1200

1201

1202

1203

1204

1205

1206

1207

1208

1209

1210

1211

1212

1213

1214

1215

1216

1217

1218

1219

1220

1221

1222

1223

1224

1225

1226

1227

1228

1229

1230

1231

1232

1233

1234

1235

1236

1237

1238

1239

1240

1241

1242

1243

1244

1245

1246

1247

1248

1249

1250

1251

1252

1253

1254

1255

1256

1257

1258

1259

1260

1261

1262

1263

1264

1265

1266

1267

1268

1269

1270

1271

1272

1273

1274

1275

1276

1277

1278

1279

1280

1281

1282

1283

1284

1285

1286

1287

1288

1289

1290

1291

specifically bacterial triacylglycerol lipase transcripts decreased in response to decomposition, while fungal triacylglycerol lipase transcripts increased. Further, expression of these genes corresponded to changes in relative abundance of the fungal classes *Saccharomycetes*, *Sordariomycetes*, and *Eurotiomycetes* [14]. These fungi have been previously associated with decomposition soils [26, 27] and are known to contain triacylglycerol lipase genes in their genomes [28, 29], suggesting that they play a role in lipid degradation in decomposition soils.

Our observation of an overall decrease in triacylglycerol lipase transcripts contrasts with previous work by Howard et al. (2010) [18], who observed increased gene copy number of Group 1 lipase genes via qPCR during swine decomposition. Fatty acid composition differs in human compared to pig tissue [30], potentially altering the lipid profile available for microbes, leading to differences in decomposition products within the soil [17]. These products can then directly or indirectly alter community composition and/or activity of functional proteins via substrate availability or the chemical environment. Further, decomposition of humans and pigs resulted in increased pH in soils below pigs, and decreased pH below humans [17]. Altered pH and soil chemistry could result in a different functional potential and/or gene expression in decomposition-impacted soils. Many triacylglycerol lipases have a pH optimum that is neutral to basic [31–33], so cells may be decreasing expression under acidic conditions in human decomposition soils. Availability of lipid species and changes to pH may select for taxa that favor these substrates/pH conditions; for example, Mason et al. (2022) [12] suggested the abundance of the fungal taxa *Saccharomycetes* was related to antemortem BMI due to relative proportions of fat and muscle tissue.

## Evidence for phased denitrification and nitrification

The human body is a concentrated source of nitrogen that is released into the surrounding soil during decomposition, therefore we also evaluated expression of genes involved

1059 in nitrogen cycling. Expression of common marker genes for nitrogen cycling was  
 1060 altered in decomposition soil and suggested nitrogen transformations during human  
 1061 decomposition are driven by soil oxygen concentrations with hydroxylamine as an  
 1062 important intermediate. We observed low or reduced expression of nitrification genes  
 1063 *nrrA* and *amoA* between days 12 and 86, during a period when oxygen was reduced to  
 1064 39% - 85%. This was concomitant with accumulation of ammonium, which reached a  
 1065 maximum on day 12, and low nitrate conditions indicating that nitrification was inhib-  
 1066 ited. This period of reduced soil oxygen constraining nitrification was also described  
 1067 in a decomposition experiment with beaver carcasses Keenan et al. (2018) [8].  
 1068 We observed increased expression of *hao*, which encodes the enzyme hydroxylamine  
 1069 dehydrogenase (HAO) at day 86 while oxygen was reduced (~85%). This corresponded  
 1070 to simultaneous increases in expression of genes encoding nitric oxide reductase (*norB*)  
 1071 and nitrous oxide reductase (*nosZ*). Traditionally HAO has been thought to pro-  
 1072 cess hydroxylamine to nitrite during nitrification, while NorB and NosZ are enzymes  
 1073 involved in the last two steps of denitrification converting nitric oxide (NO) to dini-  
 1074 trogen gas (N<sub>2</sub>). However, recent work has suggested hydroxylamine can be converted  
 1075 to nitric oxide (NO), as well as can interact with multiple phases of the nitrogen cycle  
 1076 [34]. Even though *amoA* expression was shown to decrease during reduced oxygen  
 1077 conditions, *amoA* transcripts were still present and likely able to convert ammonium  
 1078 to hydroxylamine as soil oxygen was not completely depleted during decomposition.  
 1079 Additionally, a previous study reported that the growth of the ammonia oxidizing  
 1080 bacteria *Nitrosomonas europaea* under anoxic conditions lead to accumulation of  
 1081 hydroxylamine in a chemostat bioreactor [35], suggesting anaerobic ammonium oxi-  
 1082 dation (anammox) may also be occurring in decomposition soils. However, we did  
 1083 not observe increases in *nirK* expression, which might suggest conversion of nitrite to  
 1084 NO for use in the anammox pathway. NO produced via HAO activity may be used  
 1085 for anammox in these soils; however, the role of hydroxylamine as an intermediate  
 1086



in anammox is still debated [34]. Therefore, our current hypothesis is that hydroxylamine accumulates under anaerobic conditions during decomposition, which can then be converted to NO by HAO. This NO would then be present for anaerobic denitrifying bacteria to convert to nitrous oxide (N<sub>2</sub>O) by NorB and finally to N<sub>2</sub> by NosZ. Keenan et al. (2018) [8] also noted a brief increase in N<sub>2</sub>O emissions, which suggests denitrification was occurring during this phase of reduced soil oxygen concentrations.

As soils fully reoxygenated by day 168, we observed increased expression of genes encoding enzymes involved in aerobic nitrification, *amoA* and *nxrR*. Nitrification is an oxygen-dependent process which would be converting the accumulated ammonium to nitrate; the increase in nitrate concentrations may then serve as a substrate for denitrification. We observed increased expression of marker genes encoding all four enzymes in the complete dissimilatory denitrification pathway (*narG*, *nirK*, *norB*, and *nosZ*) at day 376. Increased expression of nitrification and denitrification marker genes is consistent with accumulation of nitrite, nitrate, and N<sub>2</sub>O after oxygen is reintroduced to soils described in Keenan et al. (2018) [3, 8]. Together, gene expression patterns in our study provide further insight into nitrogen transformations in during vertebrate decomposition, suggesting an important role of hydroxylamine.

## Increased expression of bile salt hydrolases

Sulfur is present in various organic molecules, including taurine, a sulfur- and nitrogen-containing acid involved in bile acid formation [21]. Taurine is present in the human body, where it can be absorbed from the diet or synthesized in the liver [36]. However, taurine is also produced as a byproduct of the deconjugation of bile salts via bile salt hydrolases (BSH) present in the anaerobic gut taxa *Lactobacillus* and *Clostridium* [21]. In our study, we observed increased expression of genes encoding BSH enzymes between days 12 and 86. Given that increased expression of BSH genes corresponded to the beginning of active decomposition, when decomposition products were observed

1151 to enter the soil, and the period of reduced dissolved oxygen in our study, it is likely  
 1152 that taurine accumulation is the result of BSH enzyme activity by anaerobic microor-  
 1153 ganisms. While we did not measure taurine concentrations in this study, our results  
 1154 correspond to previous decomposition studies that report accumulation of taurine  
 1155 in various organs and body regions [37–39] and soils [17, 40] during decomposition  
 1156 via metabolomics, and increased relative abundance of *Clostridium* and *Lactobacillus*  
 1157 within the body [41–43] and in decomposition soils [19] via DNA sequencing methods,  
 1158 including in these soils [14].

1164  
 1165 One pathway of taurine metabolism is through desulfurization via the  $\alpha$ -ketoglutarate-  
 1166 dependent enzyme taurine dioxygenase (TauD). Specifically, this enzyme, encoded  
 1167 by the gene *tauD*, converts 2-oxoglutarate and taurine to produce aminoacetalde-  
 1168 hyde, succinate, sulfite, and CO<sub>2</sub> [44]. Succinate and sulfite from this reaction can  
 1169 then be used for the citric acid cycle and sulfur metabolism, respectively. Given  
 1170 increased BSH expression in our study and reported taurine accumulation in others,  
 1171 we would expect taurine to be present for microbial metabolism by TauD. However,  
 1172 we observed a general decrease in *tauD* expression between days 12 through 376. This  
 1173 trend was driven by reduced expression of *tauD* transcripts associated with *Proteobac-*  
 1174 *teria*, *Gammaproteobacteria*, and *Actinobacteria* whose relative abundance have been  
 1175 shown to remain consistent or increase during human decomposition [19], suggesting  
 1176 that *tauD* expression is downregulated under decomposition conditions. However, we  
 1177 noted that expression of *tauD* genes associated with fungi and a few *Betaproteobac-*  
 1178 *teria* displayed increased expression at day 58, corresponding to increased expression  
 1179 of bile salt hydrolases (BSH) between days 12 and 86. The reduction in *tauD* expres-  
 1180 sion may be due to increased sulfur availability. We did not measure sulfur species  
 1181 in this experiment; however, others have observed increased sulfur concentrations in  
 1182 decomposition-impacted soils [3, 7, 11]. Thus, sulfur scavenging pathways such as tau-  
 1183 rine desulfurization by TauD [45], whose genes are expressed under sulfur-limiting  
 1184

conditions, likely display reduced expression under sulfur replete conditions. Additionally, taurine may be processed through other pathways. For example, taurine can be deaminated by taurine dehydrogenase to produce sulfite and acetyl-CoA for carbon metabolism [44, 46]. Overall, our results suggest that human decomposition has potential impacts on soil sulfur biogeochemistry through deposition of inorganic (sulfate) and organic (sulfur-containing amino acids) sulfur compounds.

## Conclusion

This study represents the first investigation of soil microbial gene expression during human decomposition. Metatranscriptomic analysis of soils from three human individuals over one year shows that decomposition impacted microbial community gene expression profiles, exhibiting functional shifts over time. This included altered expression of genes involved in lipid, N and S metabolism as microbes processed the nutrient-rich tissues of the human body. Additionally, we noted that functionality within decomposition-impacted soils was still affected after one year and had not returned to starting or background conditions. Together, these results show that vertebrate decomposition has lasting impacts on local soil ecosystems, including soil microbial communities. These results have important implications for understanding biogeochemical changes due to vertebrate mortality events in terrestrial ecosystems.

## Materials and Methods

### Study design

In February 2018, three deceased male human subjects (hereafter, “donors”) were placed supine on the soil surface at the University of Tennessee Anthropology Research Facility (ARF) and allowed to decompose. Located in Knoxville, TN (35° 56’ 28” N, 83° 56’ 25” W) the ARF is a roughly 2-acre outdoor facility dedicated to studying

human decomposition [47]. The soils at the ARF are comprised of the Loyston-Talbott-Rock outcrop (LtD) and Coghill-Corryton (CcD) complexes. LtD soils are a silty clay loam and channery clay overlaying lithic bedrock, while CcD soils are comprised of clay from weathered quartz limestone [14, 47]. A site that had not been previously exposed to decomposition was used for this study.

The decomposition field experiment is fully described in Taylor et al. (2024) [14]. Briefly, experiments were conducted in a block design, where each block consisted of one decomposition site and one control site [14]. In total three blocks, *i.e.*, three donors paired with three respective control sites, were included in the study. Each control site was chosen in a manner to ensure their location was uphill and roughly 2 m away from decomposition sites [14]. Donor internal temperatures were recorded by probes located in the abdomen, while ambient air temperatures were monitored via sensors located roughly 50 cm above the soil surface. Soil temperature and salinity were measured with sensors placed directly underneath each individual (Decagon Devices, GS3) [14]. Donor ages ranged from 65 to 86 and were within 1 kg of each other with regard to weight (90.7 to 91.6 kg); donor BMI varied between 27.7 to 29.6 [14].

## Sampling and physiochemistry

Decomposition of all subjects was observed for one year. During the one-year study period, soils were sampled at 20 timepoints chosen to correspond with morphological stages of decomposition as described by [48]. Once advanced decay was reached, soils were collected at intervals of 350 accumulated degree days (ADD), calculated using ambient air temperatures, up to one year. All soil cores were taken using a 1.9 cm (3/4 inch) diameter soil auger to a depth of 16 cm. Soils were divided into two depth fractions: 0-1 cm (interface) and 1-16 cm (core) for the analyses reported in Taylor et al. (2024) [14]; the entire 0 to 16 cm core was used for this current study. Decomposition soils were taken from directly beneath the cadavers, taking care to not re-sample

the same location more than once. At the time of sampling, soil dissolved oxygen was measured in triplicate using an Orion Star™ A329 pH/ISE/Conductivity/Dissolved Oxygen portable multiparameter meter (ThermoFisher) [14].

A subset of 6 study timepoints were chosen for metatranscriptomics analysis. Study days 0, 12, 58, 86, 168, and 376 were chosen as they represented distinct morphological and soil biogeochemical stages during decomposition. Study day 0 was chosen as a baseline sample prior to cadaver placement. Study day 12 was the start of active decomposition and corresponded to maximum soil ammonium concentrations and minimum soil oxygen (approximately 39%). Study day 58 was chosen as this sample represented the pH minimum, and respiration and soil temperature were at a maximum [14]. Additionally, ammonium concentrations began to decrease around day 58. Study day 86 was when soil oxygen started to recover and nitrate levels began to increase. Study day 168 was chosen as nitrate was at its maximum and soil dissolved oxygen had returned to 99%. Finally, day 376 was chosen to represent the end of the study, 1 year since cadaver placement. Each study day was represented by four soil samples for RNA extraction: one pooled control sample which was a mix of the three control locations, plus one sample from each of the three donors, yielding a total of 24 samples for this study.

Soil samples were transported back to the University of Tennessee (Knoxville, TN) and processed within 24 hours of collection. Soils were homogenized by hand to remove insect larvae, roots, rocks, and other debris ( $> 2$  mm). A subset of soils were used to measure pH, electrical conductivity (EC), and evolved  $\text{CO}_2$  as described in Taylor (2024). Soil nitrogen species ( $\text{NH}_4^+$ ,  $\text{NO}_3^-$ ) and total carbon (TC) and nitrogen (TN) were measured in all soil samples as described in [14]. Reported values for soil physiochemistry represent the full 16 cm core; estimated by summing interface and core

values reported by Taylor et. al, (2024) [14] in 1:16 and 15:16 ratios, respectively. Control reported here are means of the three experimental controls that were unimpacted by decomposition.

Roughly 10 g of soil was reserved for nucleic acid extraction, placed in a 4 oz. Whirl-Pak™ bag (Nasco), and flash frozen in liquid nitrogen. All samples were stored at -80°C until further analysis. Bacterial and fungal community composition was assessed via amplicon sequencing of the 16S rRNA gene and ITS2 region as described in Taylor et al. (2024).

## RNA Extraction and Sequencing

RNA was extracted from 2 g of soil using Qiagen's RNeasy® PowerSoil® Total RNA kit. Manufacturer's instructions were followed with a few modifications. Soils became saline during decomposition; therefore, we followed the manufacturer's suggestion and incubated all extracts at -20°C following addition of solution SR4 (step 9) to decrease salt precipitation. All RNA samples were resuspended in 40 µl of Solution SR7. RNA concentrations were assessed fluorometrically using the Qubit® RNA HS assay (catalog no. Q32852) with 1 µl of RNA. DNA contamination was removed by DNase treating RNA extracts twice using Qiagen's DNase Max® kit in 50 µl reactions. RNA concentrations were remeasured after DNase treatment. PCR with V4 16S rRNA gene primers [49, 50] was conducted using RNA extracts as the template to confirm removal of all DNA prior to sequencing. RNA aliquots were shipped to HudsonAlpha Discovery (Huntsville, AL) for library preparation and RNA sequencing. Dual-indexed libraries were prepared using the Illumina® Stranded Total RNA prep with ribosomal RNA depletion via ligation with Ribo-Zero Plus. Libraries were then pooled and sequenced on Illumina's NovaSeq 6000 v4 platform, resulting in demultiplexed fastq files for each sample.

## Bioinformatics

Read quality control (QC) was conducted in KBase [51] using Trimmomatic [52]. Paired fastq files were imported to KBase through Globus. Poor quality reads were removed, and adapters trimmed via Trimmomatic (v0.36) using default settings and the TruSeq3-PE-2 adapter file. After QC check with FastQC, trimmed libraries were exported as fastq files from KBase through Globus. Remaining ribosomal RNA was filtered using bbmap (maxindel = 20, minid = 0.93) from the Joint Genome Institute's (JGI) bbtools suite [53]. After this step, all non-ribosomal reads from all 24 samples were merged into one file. This file was then used to co-assemble reads into contigs using the de novo assembler MEGAHIT (v1.2.9) [54] (-12 -k-min 23, -k-max 123, -k-step 10).

Gene identification and annotation from co-assembled contigs was performed using Prodigal [55] and eggNOG mapper [56], respectively. Briefly, the fastq containing all contigs was submitted to Prodigal (v2.6.3) for protein coding gene predication for a meta-sample (-p meta -f gff). Next, predicated genes were functionally and taxonomically annotated using eggNOG mapper (v2.1.6) using basic settings to perform a diamond blastp search [57]. Only genes that were both functionally and taxonomically annotated by one of the databases used by eggNOG mapper and identified as bacterial, archaeal, or fungal were chosen as genes of interest. Transcript counts for all genes of interest were obtained by mapping reads from each respective sample to genes of interest obtained from co-assembly using QIAGEN CLC Genomics Workbench 20.0 (<https://digitalinsights.qiagen.com/>).

## Differential Expression

Transcript counts from all samples were combined in a single workable data file and imported into R for differential expression analysis using the R packages edgeR [58]

1427 and limma [59] following a modified pipeline by Phipson et al. (2020) [60]. The tran-  
 1428 script count table was imported into R and converted to a DGElist object. Genes  
 1429 without sufficient counts for statistical analysis were removed to increase power using  
 1430 the edgeR function filterByExpr(), using study day as the comparison group.  
 1431  
 1432 Raw counts were then log2 normalized and gene expression profiles compared via  
 1433 multidimensional scaling (MDS) and hierarchical clustering. Multidimensional scaling  
 1434 (MDS) was conducted using plotMDS() from the limma package to assess differences  
 1435 between samples. MDS values were extracted from the MDS object, and the first two  
 1436 dimensions plotted using ggplot2 [61]. We also assessed the relationship between gene  
 1437 expression profiles and changes in the soil environment using canonical correspondence  
 1438 analysis (CCA). Environmental variables of interest included decomposition time in  
 1439 accumulated degree hours (ADH) based on ambient temperatures, ADH based on  
 1440 internal gut temperatures, ADH based on soil temperatures, gravimetric moisture,  
 1441 pH, electrical conductivity (EC), dissolved oxygen (DO), CO<sub>2</sub> (mol gdw<sup>-1</sup>), NH<sub>4</sub> (mg  
 1442 gdw<sup>-1</sup>), NO<sub>3</sub> (mg gdw<sup>-1</sup>), N %, C %, and CN ratio. First, permutational multivariate  
 1443 analysis of variance (PERMANOVA) with adonis() (vegan v2.6.7) [62] was used to  
 1444 identify significant soil parameters. Then the vegan functions cca() and scores() were  
 1445 applied to run the CCA and extract scores, respectively. Scores for the first two  
 1446 dimensions were plotted using ggplot2, with loadings extracted from the CCA biplot.  
 1447  
 1448 For differential expression analysis, raw filtered reads were normalized using edgeR's  
 1449 trimmed mean of M values (TMM) normalization using the function calcNormFac-  
 1450 tors(). TMM normalized reads were then log2 transformed using limma's voom() and  
 1451 differential expression assessed. Empirical Bayes shrinkage was used correct to p-  
 1452 values for false discovery rates. The topmost up and down regulated genes for each  
 1453 comparison, determined by log2 fold change and adjusted p-values, were then reported.  
 1454  
 1455 Expression of certain genes were assessed after performing transcripts per million  
 1456  
 1457  
 1458  
 1459  
 1460  
 1461  
 1462  
 1463  
 1464  
 1465  
 1466  
 1467  
 1468  
 1469  
 1470  
 1471  
 1472



(TPM) normalization and statistical analyses with a combination of analysis of variance (ANOVA) and post-hoc Tukey tests. ANOVA across all timepoints were applied to hierarchical linear mixed effects models to account for repeated sampling within each donor block.

## Availability of data and materials

RNA sequence files from the Novoseq instrument can be found at XXXX. The datasets supporting the conclusions of this article are available at the GitHub repository [Mason\\_MetaT\\_XXX\\_2024](#).”

## References

- [1] Benninger, L. A., Carter, D. O. & Forbes, S. L. The biochemical alteration of soil beneath a decomposing carcass. *Forensic Science International* **180**, 70–5 (2008).
- [2] Towne, E. G. Prairie vegetation and soil nutrient responses to ungulate carcasses. *Oecologia* **122**, 232–239 (2000). URL <https://doi.org/10.1007/PL00008851>.
- [3] DeBruyn, J. M., Keenan, S. W. & Taylor, L. S. From carrion to soil: microbial recycling of animal carcasses. *Trends in Microbiology* (2024). URL <https://doi.org/10.1016/j.tim.2024.09.003>. Publisher: Elsevier.
- [4] Parmenter, R. R. & MacMahon, J. A. Carrion decomposition and nutrient cycling in a semiarid shrub–steppe ecosystem. *Ecological Monographs* **79**, 637–661 (2009).
- [5] Macdonald, B. C. T. *et al.* Carrion decomposition causes large and lasting effects on soil amino acid and peptide flux. *Soil Biology and Biochemistry* **69**, 132–140 (2014).

1519 [6] Bump, J. K. *et al.* Ungulate carcasses perforate ecological filters and create  
1520 biogeochemical hotspots in forest herbaceous layers allowing trees a competitive  
1521 advantage. *Ecosystems* **12**, 996–1007 (2009).  
1522  
1523  
1524 [7] Aitkenhead-Peterson, J. A., Owings, C. G., Alexander, M. B., Larison, N. &  
1525 Bytheway, J. A. Mapping the lateral extent of human cadaver decomposition  
1526 with soil chemistry. *Forensic Science International* **216**, 127–34 (2012).  
1527  
1528  
1529 [8] Keenan, S. W., Schaeffer, S. M., Jin, V. L. & DeBruyn, J. M. Mortality hotspots:  
1530 nitrogen cycling in forest soils during vertebrate decomposition. *Soil Biology and*  
1531 *Biochemistry* **121**, 165–176 (2018).  
1532  
1533  
1534 [9] Fancher, J. P. *et al.* An evaluation of soil chemistry in human cadaver decom-  
1535 position islands: Potential for estimating postmortem interval (PMI). *Forensic*  
1536 *Science International* **279**, 130–139 (2017).  
1537  
1538  
1539 [10] Quaggiotto, M.-M., Evans, M. J., Higgins, A., Strong, C. & Barton, P. S.  
1540 Dynamic soil nutrient and moisture changes under decomposing vertebrate  
1541 carcasses. *Biogeochemistry* **146**, 71–82 (2019).  
1542  
1543  
1544 [11] Taylor, L. S. *et al.* Soil elemental changes during human decomposition.  
1545 *PLoS ONE* **18**, 1–24 (2023). URL <https://doi.org/10.1371/journal.pone.0287094>.  
1546  
1547  
1548 Publisher: Public Library of Science.  
1549  
1550  
1551 [12] Mason, A. R. *et al.* Body mass index (BMI) impacts soil chemical and microbial  
1552 response to human decomposition. *mSphere* e0032522 (2022).  
1553  
1554  
1555 [13] Mason, A. R., Taylor, L. S. & DeBruyn, J. M. Microbial ecology of vertebrate  
1556 decomposition in terrestrial ecosystems. *FEMS Microbiology Ecology* **99**, fiad006  
1557  
1558  
1559 (2023). URL <https://doi.org/10.1093/femsec/fiad006>.  
1560  
1561  
1562  
1563  
1564

- [14] Taylor, L. S. *et al.* Transient hypoxia drives soil microbial community dynamics and biogeochemistry during human decomposition. *FEMS Microbiology Ecology* **100**, fae119 (2024). URL <https://doi.org/10.1093/femsec/fae119>.
- [15] Burcham, Z. M. *et al.* Total RNA analysis of bacterial community structural and functional shifts throughout vertebrate decomposition. *Journal of Forensic Sciences* **64**, 1707–1719 (2019).
- [16] Ashe, E. C., Comeau, A. M., Zejdlik, K. & O’Connell, S. P. Characterization of bacterial community dynamics of the human mouth throughout decomposition via metagenomic, metatranscriptomic, and culturing techniques. *Frontiers in Microbiology* **12**, 689493 (2021).
- [17] DeBruyn, J. M. *et al.* Comparative decomposition of humans and pigs: soil biogeochemistry, microbial activity and metabolomic profiles. *Frontiers in Microbiology* **11**, 608856 (2021).
- [18] Howard, G. T., Duos, B. & Watson-Horzelski, E. J. Characterization of the soil microbial community associated with the decomposition of a swine carcass. *International Biodeterioration & Biodegradation* **64**, 300–304 (2010).
- [19] Cobaugh, K. L., Schaeffer, S. M. & DeBruyn, J. M. Functional and structural succession of soil microbial communities below decomposing human cadavers. *Plos One* **10**, e0130201 (2015).
- [20] Singh, B. *et al.* Temporal and spatial impact of human cadaver decomposition on soil bacterial and arthropod community structure and function. *Frontiers in Microbiology* **8**, 2616 (2018).
- [21] Urdaneta, V. & Casadesús, J. Interactions between Bacteria and Bile Salts in the Gastrointestinal and Hepatobiliary Tracts. *Frontiers in Medicine* **4** (2017).

1611 [22] van der Wal, A., Geydan, T. D., Kuyper, T. W. & de Boer, W. A thready affair:  
1612 linking fungal diversity and community dynamics to terrestrial decomposition  
1613 processes. *FEMS Microbiology Reviews* **37**, 477–494 (2013).  
1614  
1615  
1616  
1617 [23] Essington, M. E. *Soil and water chemistry: an integrative approach* (CRC press,  
1618 2015).  
1619  
1620  
1621 [24] Peng, J., Wegner, C.-E. & Liesack, W. Short-term exposure of paddy soil micro-  
1622 bial communities to salt stress triggers different transcriptional responses of key  
1623 taxonomic groups. *Frontiers in Microbiology* **8** (2017).  
1624  
1625  
1626  
1627 [25] Pandit, A. S. *et al.* A snapshot of microbial communities from the Kutch: one of  
1628 the largest salt deserts in the World. *Extremophiles* **19**, 973–987 (2015).  
1629  
1630  
1631 [26] Metcalf, J. L. *et al.* Microbial community assembly and metabolic function during  
1632 mammalian corpse decomposition. *Science* **351**, 158–62 (2016).  
1633  
1634  
1635 [27] Fu, X. *et al.* Fungal succession during mammalian cadaver decomposition and  
1636 potential forensic implications. *Scientific Reports* **9**, 12907 (2019).  
1637  
1638  
1639 [28] Dujon, B. *et al.* Genome evolution in yeasts. *Nature* **430**, 35–44 (2004).  
1640  
1641  
1642 [29] Haridas, S. *et al.* The genome and transcriptome of the pine saprophyte *Ophios-*  
1643 *toma piceae*, and a comparison with the bark beetle-associated pine pathogen  
1644 *Grosmannia clavigera*. *BMC Genomics* **14**, 373 (2013).  
1645  
1646  
1647  
1648 [30] Notter, S. J., Stuart, B. H., Rowe, R. & Langlois, N. The initial changes of fat  
1649 deposits during the decomposition of human and pig remains. *Journal of Forensic*  
1650 *Sciences* **54**, 195–201 (2009).  
1651  
1652  
1653 [31] Kok, R. G. *et al.* Characterization of the extracellular lipase, LipA, of *Acineto-*  
1654 *bacter calcoaceticus* BD413 and sequence analysis of the cloned structural gene.  
1655  
1656

- Molecular Microbiology* **15**, 803–818 (1995). 1657  
1658
- [32] Hasan, F., Shah, A. A. & Hameed, A. Influence of culture conditions on lipase 1659  
production by *Bacillus* sp. FH5. *Annals of Microbiology* **56**, 247–252 (2006). 1660  
1661  
1662  
1663
- [33] Zouaoui, B. & Bouziane, A. Production, optimization and characterization of 1664  
the lipase from *Pseudomonas aeruginosa*. *Romanian biotechnological letters* **17**, 1665  
7187–7193 (2012). 1666  
1667  
1668
- [34] Soler-Jofra, A., Pérez, J. & van Loosdrecht, M. C. M. Hydroxylamine and the 1669  
nitrogen cycle: A review. *Water Research* **190**, 116723 (2021). 1670  
1671  
1672  
1673
- [35] Yu, R., Perez-Garcia, O., Lu, H. & Chandran, K. *Nitrosomonas europaea* adapta- 1674  
tion to anoxic-oxic cycling: Insights from transcription analysis, proteomics and 1675  
metabolic network modeling. *Science of the Total Environment* **615**, 1566–1573 1676  
(2018). 1677  
1678  
1679  
1680
- [36] Seidel, U., Huebbe, P. & Rimbach, G. Taurine: A regulator of cellular redox 1681  
homeostasis and skeletal muscle function. *Molecular Nutrition & Food Research* 1682  
**63**, 1800569 (2019). 1683  
1684  
1685  
1686
- [37] Mora-Ortiz, M., Trichard, M., Oregioni, A. & Claus, S. P. Thanatometabolomics: 1687  
introducing NMR-based metabolomics to identify metabolic biomarkers of the 1688  
time of death. *Metabolomics* **15**, 37 (2019). 1689  
1690  
1691  
1692
- [38] Locci, E. *et al.* A <sup>1</sup>H NMR metabolomic approach for the estimation of the time 1693  
since death using aqueous humour: an animal model. *Metabolomics* **15**, 76 (2019). 1694  
1695  
1696
- [39] Zelentsova, E. A. *et al.* Post-mortem changes in the metabolomic compositions 1697  
of rabbit blood, aqueous and vitreous humors. *Metabolomics* **12**, 172 (2016). 1698  
1699  
1700  
1701  
1702

1703 [40] Hoeland Katharina, M. *Investigating the potential of postmortem metabolomics*  
1704 *in mammalian decomposition studies in outdoor settings*. Ph.D. thesis, University  
1705 of Tennessee-Knoxville, [https://trace.tennessee.edu/utk\\_graddiss/7000](https://trace.tennessee.edu/utk_graddiss/7000) (2021).  
1706  
1707  
1708  
1709 [41] Javan, G. T. *et al.* Human thanatobiome succession and time since death.  
1710 *Scientific Reports* **6**, 29598 (2016).  
1711  
1712  
1713 [42] Javan, G. T., Finley, S. J., Smith, T., Miller, J. & Wilkinson, J. E. Cadaver  
1714 thanatobiome signatures: the ubiquitous nature of Clostridium species in  
1715 human decomposition. *Frontiers in Microbiology* **8**, 2096 (2017).  
1716  
1717  
1718  
1719 [43] DeBruyn, J. M. & Hauther, K. A. Postmortem succession of gut microbial  
1720 communities in deceased human subjects. *Peerj* **5**, e3437 (2017).  
1721  
1722  
1723 [44] Cook, A. M. & Denger, K. Metabolism of taurine in microorganisms. *Taurine* **6**  
1724 3–13 (2006).  
1725  
1726  
1727 [45] Kertesz, M. A. Riding the sulfur cycle – metabolism of sulfonates and sul-  
1728 fate esters in Gram-negative bacteria. *FEMS Microbiology Reviews* **24**, 135–175  
1729 (2000).  
1730  
1731  
1732  
1733 [46] Brüggemann, C., Denger, K., Cook, A. M. & Ruff, J. Enzymes and genes of  
1734 taurine and isethionate dissimilation in Paracoccus denitrificans. *Microbiology*  
1735 *(Reading, England)* **150**, 805–816 (2004).  
1736  
1737  
1738  
1739 [47] Keenan, S. W. *et al.* Spatial impacts of a multi-individual grave on microbial  
1740 and microfaunal communities and soil biogeochemistry. *PLoS One* **13**, e0208845  
1741 (2018).  
1742  
1743  
1744  
1745 [48] Payne, J. A. A summer carrion study of the baby pig *Sus Scrofa* Linnaeus.  
1746 *Ecology* **46**, 592–602 (1965).  
1747  
1748

- [49] Apprill, A., McNally, S., Parsons, R. & Weber, L. Minor revision to V4 region SSU rRNA 806R gene primer greatly increases detection of SAR11 bacterioplankton. *Aquatic Microbial Ecology* **75**, 129–137 (2015). 1749–1754
- [50] Parada, A. E., Needham, D. M. & Fuhrman, J. A. Every base matters: assessing small subunit rRNA primers for marine microbiomes with mock communities, time series and global field samples. *Environmental Microbiology* **18**, 1403–14 (2016). 1755–1761
- [51] Arkin, A. P. *et al.* KBase: The United States Department of Energy Systems Biology Knowledgebase. *Nature Biotechnology* **36**, 566–569 (2018). 1762–1765
- [52] Bolger, A. M., Lohse, M. & Usadel, B. Trimmomatic: a flexible trimmer for Illumina sequence data. *Bioinformatics* **30**, 2114–2120 (2014). 1766–1769
- [53] Bushnell, B. BBMap. URL [sourceforge.net/projects/bbmap/](https://sourceforge.net/projects/bbmap/). 1770–1771
- [54] Li, D., Liu, C.-M., Luo, R., Sadakane, K. & Lam, T.-W. MEGAHIT: an ultra-fast single-node solution for large and complex metagenomics assembly via succinct de Bruijn graph. *Bioinformatics* **31**, 1674–1676 (2015). 1772–1777
- [55] Hyatt, D. *et al.* Prodigal: prokaryotic gene recognition and translation initiation site identification. *BMC Bioinformatics* **11**, 119 (2010). 1778–1781
- [56] Cantalapiedra, C. P., Hernández-Plaza, A., Letunic, I., Bork, P. & Huerta-Cepas, J. eggNOG-mapper v2: functional annotation, orthology assignments, and domain prediction at the metagenomic scale. *Molecular Biology and Evolution* **38**, 5825–5829 (2021). 1782–1789
- [57] Buchfink, B., Reuter, K. & Drost, H.-G. Sensitive protein alignments at tree-of-life scale using DIAMOND. *Nature Methods* **18**, 366–368 (2021). 1790–1793

- 1795 [58] Robinson, M. D., McCarthy, D. J. & Smyth, G. K. edgeR: a Bioconduc-  
 1796 tor package for differential expression analysis of digital gene expression data.  
 1797 *Bioinformatics* **26**, 139–140 (2010).  
 1798  
 1800 [59] Smyth, G. K. in *limma: Linear Models for Microarray Data* (eds Gentleman,  
 1801 R., Carey, V. J., Huber, W., Irizarry, R. A. & Dudoit, S.) *Bioinformatics and*  
 1802 *Computational Biology Solutions Using R and Bioconductor* 397–420 (Springer  
 1803 New York, New York, NY, 2005).  
 1804  
 1805 [60] Phipson, B. *et al.* Differential expression analysis (2020). URL [https://combine-](https://combine-australia.github.io/RNAseq-R/06-rnaseq-day1.html#References)  
 1806 [australia.github.io/RNAseq-R/06-rnaseq-day1.html#References](https://combine-australia.github.io/RNAseq-R/06-rnaseq-day1.html#References).  
 1807  
 1808 [61] Wickham, H. *ggplot2: Elegant Graphics for Data Analysis* (Springer-Verlag New  
 1809 York, 2016). URL <https://ggplot2.tidyverse.org>.  
 1810  
 1811 [62] Oksanen, J. *et al.* *vegan: Community Ecology Package* (2024). URL [https://](https://vegandevs.github.io/vegan/)  
 1812 [vegandevs.github.io/vegan/](https://vegandevs.github.io/vegan/).  
 1813  
 1814  
 1815  
 1816  
 1817  
 1818  
 1819  
 1820

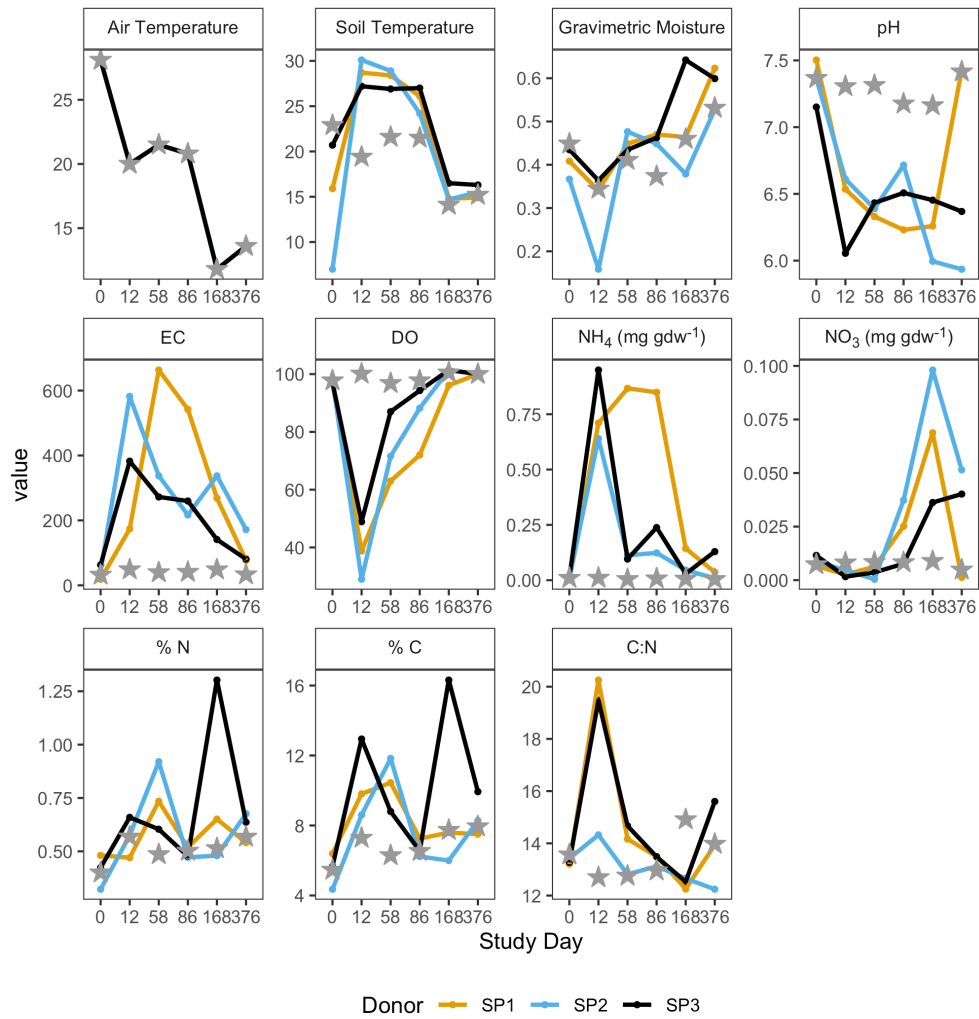
## 1821 Acknowledgements

1822 We would like to thank the Forensic Anthropology Center at the University of  
 1823 Tennessee-Knoxville for their help in setting up field experiments. We would like to  
 1824 thank Mary Davis for her help in managing the field site and helping to obtain donors  
 1825 for this work. This research was funded by a National Institute of Justice Award  
 1826 (DOJ-NIJ-2017-R2-CX-0008) to LST and JMD.  
 1827  
 1828  
 1829  
 1830  
 1831  
 1832

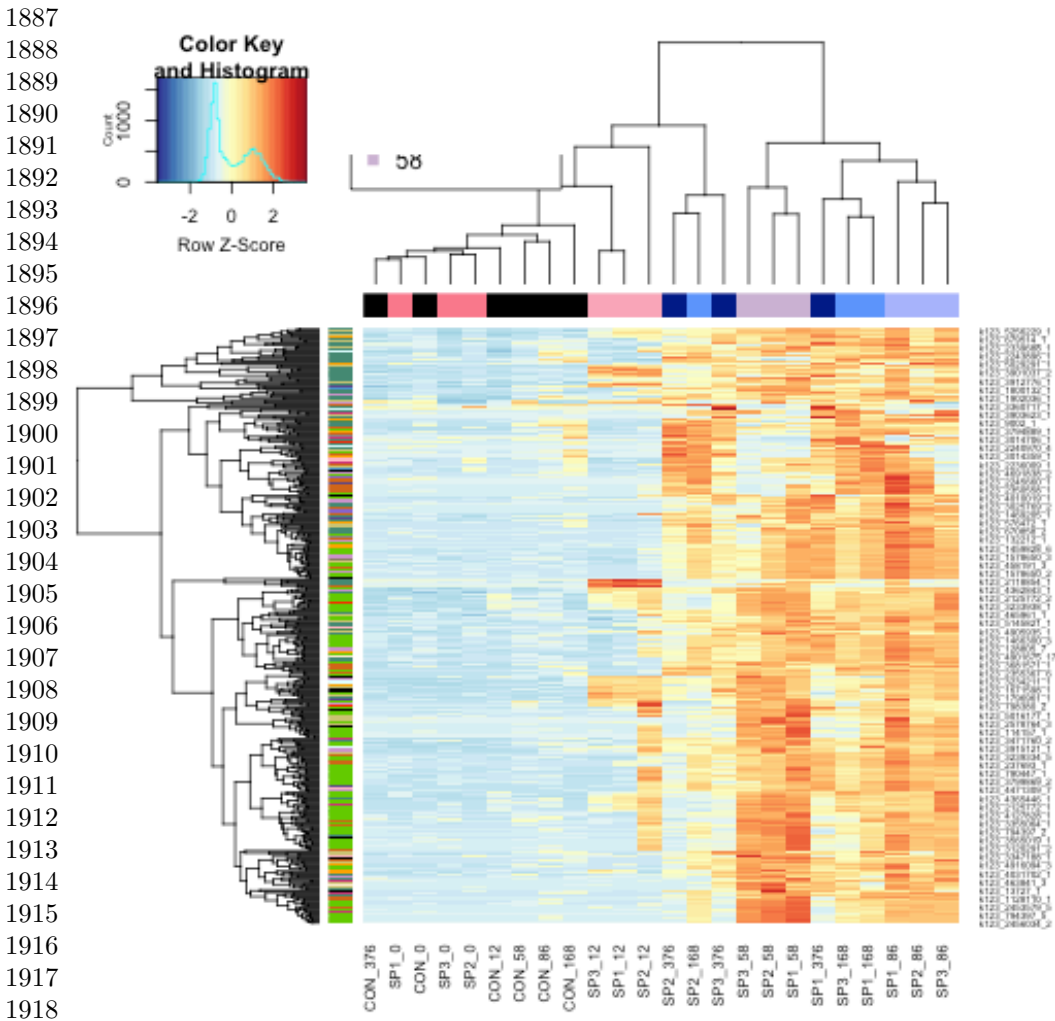
## 1833 Supplementary Information

1834  
 1835  
 1836  
 1837  
 1838  
 1839  
 1840





Supplementary Material 1: Figure S1. Soil physiochemical parameters in decomposition soils during the one-year study. Data is shown for each individual donor: SP1 (gold), SP2 (blue), and SP2 (black). Values for the full 16 cm core samples were estimated by summing values interface (0-1 cm) and core (0-16 cm) reported by Taylor et al, (2024) in 1:16 and 15:16 ratios, respectively. Controls reported here are means of three experimental controls that were unimpacted by decomposition and are represented by stars.

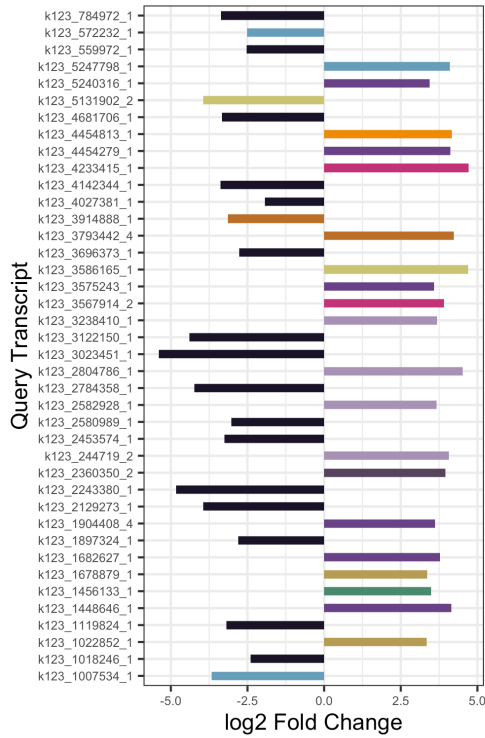


Supplementary Material 2: Figure S2. Hierarchical clustering heatmap showing the log counts per million (CPM) of the top 500 most variable genes across samples. Variable genes were determined by selecting genes with the highest variance in gene expression. Samples are clustered along the x-axis using Euclidean distances between samples and colored by study day.

Table S1. Permutational analysis of variance (PERMANOVA) results identifying significant environmental parameters which explain some of the variation in soil gene expression profiles. Environmental parameter data is from Taylor et al. (2024). Variables with  $p < 0.05$  are indicated in bold.

Supplementary Material 3

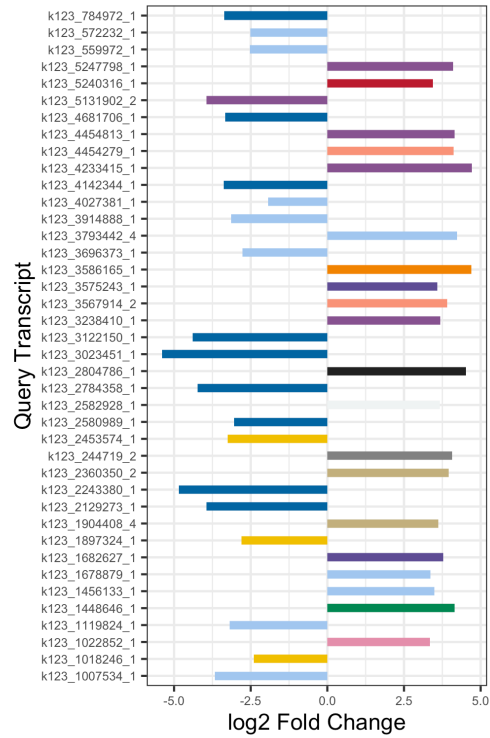
A



## COG Category

- Cell motility
- Energy production and conversion
- Transcription
- Cell cycle control, cell division, chromosome partitioning
- Carbohydrate transport and metabolism
- Intracellular trafficking, secretion and vesicular transport
- Signal transduction mechanisms
- Translation, ribosomal structure and biogenesis
- Post-translational modification, protein turnover, and ch:
- Function Unknown
- unclassified

B



## Taxonomy

- 1117|Cyanobacteria
- 1236|Gammaproteobacteria
- 135614|Xanthomonadales
- 2|Bacteria
- 200940|Thermodesulfobacteria
- 201174|Actinobacteria
- 203682|Planctomycetes
- 204432|Acidobacteriia
- 2157|Archaea
- 28211|Alphaproteobacteria
- 28221|Deltaproteobacteria
- 4751|Fungi
- 57723|Acidobacteria
- 976|Bacteroidetes

Supplementary Material 4: Figure S3. Top 40 up- and down-regulated genes in controls relative to decomposition soils across all study days, colored by COG functional category (A) and taxonomic annotation (B). Positive values denote higher expression in controls, while negative values are higher in decomposition soils.

1933  
1934  
1935  
1936  
1937  
1938  
1939  
1940  
1941  
1942  
1943  
1944  
1945  
1946  
1947  
1948  
1949  
1950  
1951  
1952  
1953  
1954  
1955  
1956  
1957  
1958  
1959  
1960  
1961  
1962  
1963  
1964  
1965  
1966  
1967  
1968  
1969  
1970  
1971  
1972  
1973  
1974  
1975  
1976  
1977  
1978

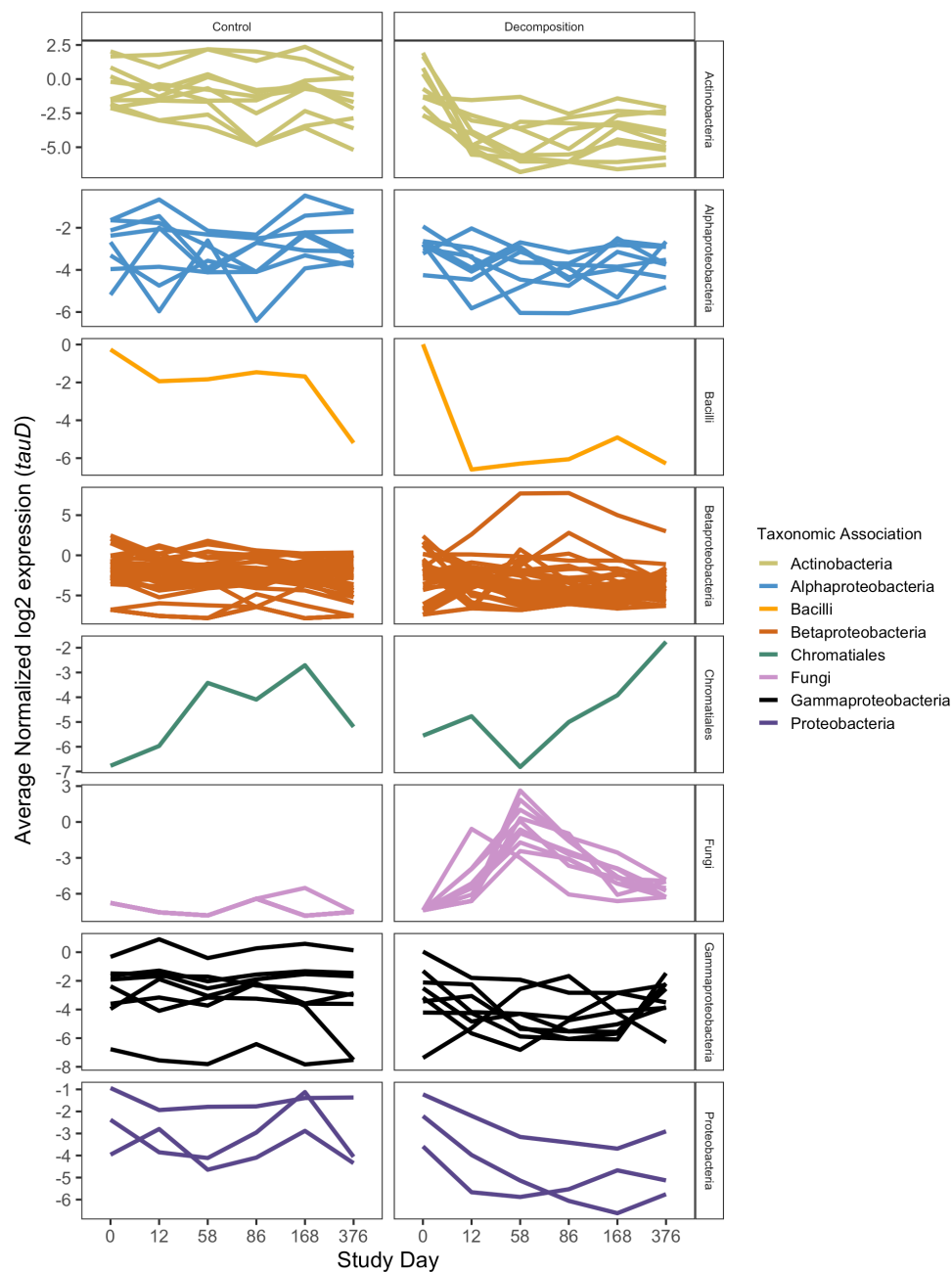
1979  
1980  
1981  
1982  
1983  
1984  
1985  
1986  
1987  
1988  
1989  
1990  
1991  
1992  
1993  
1994  
1995  
1996  
1997  
1998  
1999  
2000  
2001  
2002  
2003  
2004  
2005  
2006  
2007  
2008  
2009  
2010  
2011  
2012  
2013  
2014  
2015  
2016  
2017  
2018  
2019  
2020  
2021  
2022  
2023  
2024

Table S2. Top 20 most up- and down-regulated gene queries, determined by log2 fold change and adjusted p-values, in control relative to decomposition soils. Positive log2 fold change values represent genes whose expression was higher in control soils, while negative log2 fold change values were higher in decomposition soils. Taxonomic annotation, COG categories, gene description, gene names, and EC were assigned via eggNOG-mapper.

Supplementary Material 5

Table S3. Top 10 most up- and down-regulated genes, determined by log2 fold change and adjusted p-values, for each sequential timepoint comparison. Positive log2 fold change values represent genes whose expression was higher in the later decomposition timepoint soils, while negative log2 fold change values are higher in earlier decomposition timepoint soils. Taxonomic annotation, COG categories, gene names, and EC were assigned via eggNOG-mapper. The comparison column distinguishes each timepoint comparison.

Supplementary Material 6



Supplementary Material 7: Figure S4. Mean normalized log<sub>2</sub> expression of *tauD* genes by taxonomic association (color) in control and decomposition soils at each study day. Each line represents one *tauD* gene query, while color denotes taxonomic association as determined by eggNOG-mapper.